Atomic Resolution Coherent X-ray Imaging with Phase Retrieval:

Incorporating Changes in Temperature

Abigail Mae Hardy Carpenter

A senior thesis submitted to the faculty of
Brigham Young University
in partial fulfillment of the requirements for the degree of

Bachelor of Science

Richard Sandberg, Advisor

Department of Physics and Astronomy

Brigham Young University

ABSTRACT

Atomic Resolution Coherent X-ray Imaging with Phase Retrieval:
Incorporating Changes in Temperature

Abigail Mae Hardy Carpenter
Department of Physics and Astronomy, BYU
Bachelor of Science

In order to better understand material failure at the atomic level we study the crystalline structure of such materials at synchotrons. The new 4th-generation synchrotron sources and their increased brilliance promise to improve such measurements, as well as increase the amount of data that will need to be processed. In order to be prepared for this change, new, faster computational methods for reconstructing these grains is necessary. In this work, we present an algorithm which incorporates less computationally expensive methods of reconstruction than phase retrieval by integrating molecular dynamics into Bragg coherent diffraction imaging as well as constraining the solution using physical information. This algorithm is called PRAMMol (Phase Retrieval with Atomic Modeling and Molecular Dynamics). We show that this method successfully reconstructs simulated crystals from coherent diffraction from 3D crystals and show the correct solution to the atomic scale from 0 to 1000 K.

Keywords: Computational Methods, Optical Physics, Materials Modeling, Coherence X-Ray Scattering

ACKNOWLEDGMENTS

I would like to thank Professor Richard Sandberg for his years of mentoring and Jason Meziere for letting me tag along on his project. This work was supported by the DOE Office of Science (Office of Basic Energy Sciences)(Award number DE-SC0022133) and Argonne National Laboratory operated by DOE Office of Science User Facility operated under Contract No. AC02-06CH11357.

Contents

List of Figures

Chapter 1

Introduction

In physics, we often deal with and probe system failures. We want to know how and why things break, and these failures often are initiated on the atomic scale. The decline in battery performance is often due to lattice distortion, cracking, or the formation of harmful structures such as dendrites [1]. This occurs from the repeated stress of the charge/discharge cycles [2]. On a larger scale, hip replacements are expected to last around 25 years due to many factors including fracturing and loosing caused by wear at the atomic level [3]. Heart stent displacements could also be caused by a material failure at the atomic level [4].

At synchrotrons, we probe the crystal structure of such materials to understand these failures. This paper will focus on coherent x-ray imaging techniques to accomplish this goal. The performance of coherent x-ray imaging is expected to greatly improve down to the nanoscale level due to the new 4th-generation synchrotron sources and their increased brilliance [5]. These changes will increase the amount of data collected during runs and in turn, increase the amount of data that needs to be processed. In order to handle these increases, faster and more efficient algorithms will be necessary to reconstruct the original crystalline structure in a timely and accurate manner.

1.1 Bragg Coherent Diffraction Imaging

Bragg coherent diffraction imaging (BCDI) is a lens-less imaging technique that utilizes diffracted x-rays, electrons, or visible light to image an object. See Figure 1.1. X-ray beams enter a crystal and go through it with each atom producing a spherical wave that shows where the atoms are placed. We gather these x-rays and their information by placing detectors at a specific angle — called the Bragg angle — that shows us this bouncing best. The detectors typically see a fringe pattern — similar to a bullseye. These fringes are used to reconstruct the original crystal structure using advanced algorithms. BCDI is particularly useful for reconstructing the 3-dimensional density of a sample in a non-destructive way. Additionally, such imaging allows for the determination of the internal crystalline strain of the object. In Meziere *et al.*, a new algorithm for reconstruction is proposed and tested on simulated crystals [7].

1.2 Previous Work on Phase Retrieval

Traditional BCDI image reconstruction uses error reduction (ER) or hybrid input-output (HIO) algorithms [8,9]. These iterative methods rely heavily on two key constraints: the modulus constraint, which enforces agreement between the reconstructed Fourier magnitudes and the experimentally measured diffraction intensities, and the support constraint, which limits the object's extent in real space. As described in Fienup's foundational work, these constraints help guide the iterative process toward physically meaningful solutions, particularly in the presence of phase ambiguity. This paper presents a new algorithm that was previously published in Meziere's paper that utilizes some of the traditional BCDI image reconstruction. This algorithm includes physical model informed BCDI and is called Phase Retrieval with Atomic Modeling and Molecular Dynamics (PRAMMol) . PRAMMol fits the atomic positions to the diffraction pattern using the molecular dynamic

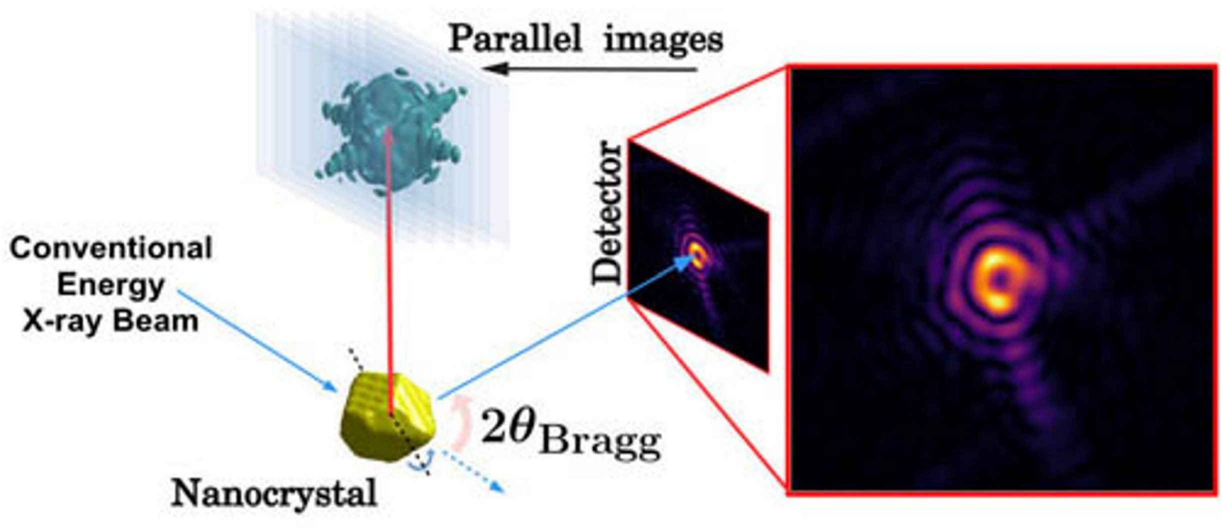

Figure 1.1
Schematic of the operating principles of BCDI. X-ray beams enter the crystal and pass through scattering off of the atoms inside. On the other sides of the crystal, detectors are placed at the Bragg angle to measure the x-rays that emerge. From the fringe patterns, we are able to reconstruct the 3-dimensional structure of the crystal using the process discussed in this paper [6].

information. Molecular dynamics simulations predict how every atom in a molecular system will move over time, based on a general model of the physics governing interatomic interactions [10].

This research has been published in the *npj Computational Materials* article "Atomic resolution coherent x-ray imaging with physics-based phase retrieval" by Jason Meziere, Abigail Hardy Carpenter, Anastasios Pateras, Ross Harder, and Richard L. Sandberg [7]. Please refer to this paper for further descriptions of the experiment.

I did not contribute to everything in this project. I worked alongside Jason to debug the original code and build some of the 0 K reconstructions. For the temperature project, I wrote parts of the code, debugged with Jason, and ran about half of the reconstructions. This code completed reconstructions with a higher accuracy compared to other reconstruction algorithms, and it performed with comparable accuracy at higher temperatures. These reconstructions were simulated to mirror atomic vibrations at 100 K, 300 K, 700 K, and 1000 K.

The focus of this thesis is to further discuss the inclusion of temperature into this algorithm and how PRAMMol still recreates accurate data. I will begin with some background on the methods behind PRAMMol including the maximum likelihood estimation, atomic generation, cross-validation, and grain creation. I will then discuss how I updated PRAMMol to better simulate the vibration of the grain due to temperature and show that this method is precise to a tenth of an Angstrom at room temperature. This method will be very useful for analyzing data from the updated synchrotrons.

Chapter 2

Methods

Many of the details and figures in this section come from Meziere *et al.* [7]. This section will discuss how the PRAMMol code works and how we used it to recreate grains while bypassing the phase retrieval problem. This allows the grain to be reconstructed quickly. PRAMMol includes principles of maximum likelihood estimation, atom generation, and cross-validation. This section will also discuss how I created simulated grains with the associated temperature vibrations and the resultant diffraction patterns that we used to test the efficiency of PRAMMol.

2.1 PRAMMol

The PRAMMol algorithm (Phase Retrieval with Atomic Modeling and Molecular Dynamics) bypasses the phase retrieval issue. It fits the atomic positions to the diffraction pattern by merging molecular dynamics and statistical techniques. It assumes the intensity of the beam and the position of the atoms using Miller indices [11]. However, there are several things that PRAMMol does not incorporate including Ewald sphere curvature and kinematic diffraction limit [12]. It also neglects multiple scattering, absorption, or dynamical diffraction. Our team disregards these because the crystal is small enough not to expect such issues. We also leave out detector pixel size and detector

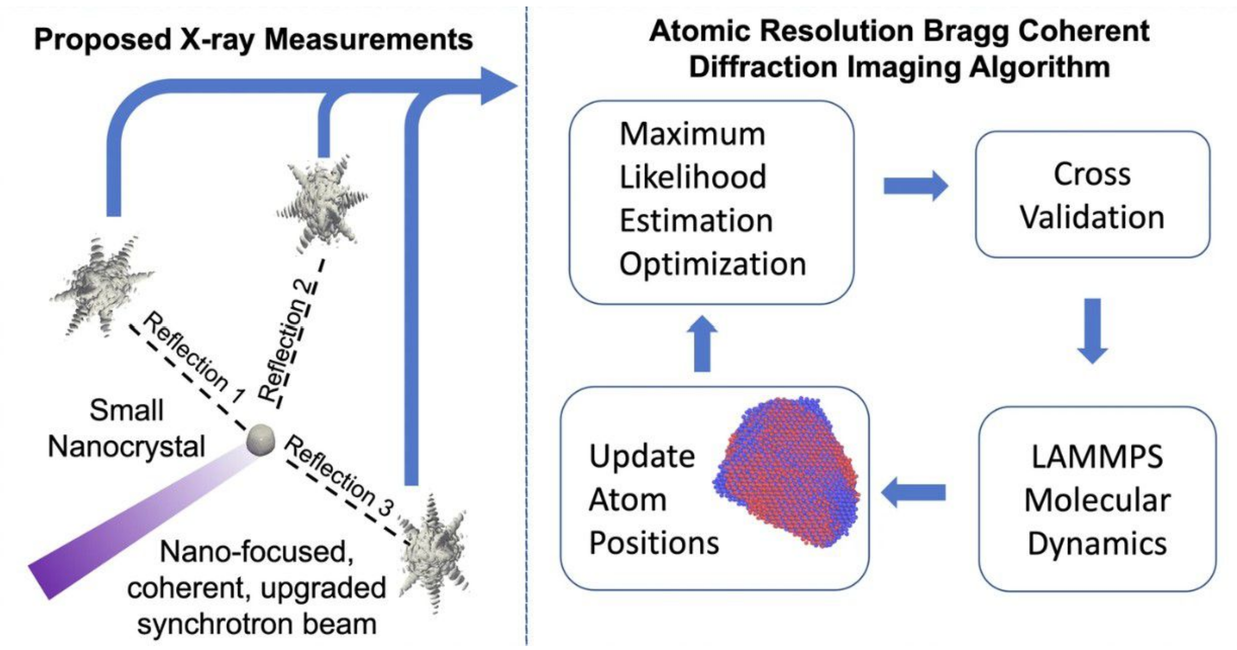

Figure 2.1
PRAMMol algorithm's process. Using 3 separate diffraction patterns, we reconstruct the crystal structure. This reconstruction occurs in three steps: maximum likelihood estimation, cross-validation, and molecular dynamics energy minimization. Through this process, an initial guess is refined so that its three diffraction patterns match those of the original crystal [7].

orientation since we are simulating the crystal rather than using real-world data. This disregard will need to be addressed further in future work on real data, and we will follow the methods discussed in the literature at that point [6, 13, 14]. However, we propose that this disregard is not significant for our experimentally simulated crystals and would be difficult to factor in due to their negligible impact. PRAMMol uses cross-validation, maximum likelihood estimation, and atom generation. They will be discussed below.

2.2 Maximum Likelihood Estimation

Maximum likelihood estimates (ML) are excellent at estimating the value of the parameters when given the data being sampled. It has previously been successfully applied to phase retrieval problems in ptychography, holography, and speckle imaging [15–17]. ML works to move the atoms to where the current pattern best matches the real diffraction pattern.

This method is unsuccessful alone since the ML is unable to change the number of atoms and tends to get stuck in the local minimum. These error local minima are actually maximum energy states, but I will call them minima in this paper for the purposes of easier visualization. These locations may have atoms in not physically realistic locations, such as overlapping with other atoms or separated from the rest of the crystal [7].

2.3 Atom Generation

In order to create new atoms and their positions, we use three different methods: Delaunay triangulation, force calculations, and random placement.

Delaunay triangulations test where to add new atoms. It begins by taking four atoms to form a tetrahedron. If this tetrahedron does not cross any other formed tetrahedrons, an atom will be added to the center of the tetrahedron. This process ensures that atoms are added no closer than the radius of the atom within this region. This effectively adds atoms to most of the empty positions within a crystal.

Force calculations allow us to calculate the force on the atoms to see if they are physically realistic. If there is an atom missing from the middle of a crystal, the ML will tend to place the atoms around the void closer to each other to better simulate the diffraction pattern. This will result in too much Coloumb interatomic force on the atoms pointing towards the location of the missing atom. This force enters into our simulations based on our molecular statics calculations [18]. At this point, we can add the missing atom in the center. The next round of the ML will fix the location of the atoms that were pulled into the void.

The Delaunay triangulations and force calculations may not perfectly place every atom. To help with this, we also randomly place atoms outside but close to the currently proposed crystal structure. This allows for the Delaunay triangulations and force calculations to better find the edge of the object in subsequent attempts.

2.4 Cross-Validation

Cross-validation seeks to find the most likely reconstruction that can create the same diffraction pattern as the one we are trying to reconstruct [19]. ML and atom generation create several different models of the atomic positions, and cross-validation compares the simulated diffraction patterns from the various proposed atomic positions with the true or measured diffraction pattern. It then selects the atomic positions that produce the lowest error comparing the proposed and true diffraction patterns.

Due to the multitude of atoms and proposed models, the cross-validation step does not actually search them all. It moves across the possibilities in a row and column pattern and seeks to find the minimum by moving one space "downhill" at a time. This is similar to how a ball rolls its way downhill; such a ball could get stuck in a trench instead of making it all the way to the bottom of a hill. This can present issues for getting stuck in the local minimum. This issue is overcome by performing cross-validation, ML, and atom generation iteratively until the first iteration when the likelihood does not change with multiple different starting points. This can be thought of like sending multiple balls down the hill. While some may get caught in trenches, not all of them will get stuck in the same trench, and after we realize there is a trench, we can send the ball down the hill in a way to avoid the trenches. The multiple balls in our analogy represent the different models formed by how we generate atoms. See Section 2.3 above.

We avoid some of the trenches or local minima by filtering. We filter to ensure that atoms are not too close together or too far apart. Atoms that are too close together would overlap in a way that is not physically possible, and atoms that are too far apart would have too much potential energy. This filtering comes from using Molecular Statics to minimize the energy and then high energy atoms are removed [18]. Too much energy would lead a proposed crystal structure to collapse in the real world. The algorithm removes about half of the atoms that are too energetic and all of the atoms that are too close together. This removal of only about half of the energetic atoms may be surprising since it may be tempting to remove all such atoms, but this partial removal allows the algorithm to escape local minima caused by too much energy without heading straight into other minima caused by too little energy.

2.5 Grain Creation

In order for us to verify that these models work, we needed to create a few simulated samples and calculate their simulated diffraction patterns. We call this grain creation. We initiated the PRAMMol method with the diffraction patterns and compared the atom positions in the grain to the structure the model is recreating to see how many steps it takes to create an accurate reconstruction.

This works by producing a list of atom positions that are hopefully the real atom positions in the grain. We do this by assuming that atoms are spheres from molecular dynamics.

We generate these test grains using a LAMMPS package called atomsk [20]. Atomsk aims at creating, manipulating, and converting atomic systems. We followed the tutorial on the website to create a sample with no defects, a sample with a single atom removed (vacancy), and a sample with a screw dislocation. We then minimized the energy using LAMMPS to bring the samples to a steady state [21–23]. Large-scale Atomic/Molecular Massively Parallel Simulator (LAMMPS) is a classical molecular dynamics code with a focus on materials modeling.

To create the diffraction patterns, we calculate the $(\bar{1},1,1)$, $(1,\bar{1},1)$, and $(1,1,\bar{1})$ peaks. We then applied a Poisson distribution to find the *h,k* and *l*. See Equations 2.1 and 2.2 below. Thus we created the diffraction pattern.

$$I_{hkl} \overset{\text{ind}}{\sim} Pois(\lambda_{hkl}(C,\vec{x},\vec{y},\vec{z})) \tag{2.1}$$

$$\lambda_{hkl}(C,\vec{x},\vec{y},\vec{z}) = |F_{hkl}|^2 = \left| \sum_{j=1}^{n} Ce^{-2\pi i(hx_j+ky_j+lz_j)} \right|^2 \tag{2.2}$$

For the equations above, n is the number of atoms in the sample, F_{hkl} is the structure factor and is proportional to the electric field at the detector, C is an unknown scaling constant that describes the TIPF and several other experimental factors, and (hx_j, ky_j, lz_j) is the j^{th} of n atomic positions in the material being imaged. In this formulation, the atomic positions and scaling constant become parameters of a family of probability density functions [7].

2.6 Temperature-dependent diffraction pattern

The initial PRAMMol method used grains and their corresponding Bragg peaks had been relaxed at 0 K [7]. This is not physically realistic, so we wanted to add temperature to all three generated samples to better simulate the vibration of the atoms. At 0 K, atoms have no kinetic energy, so they do not vibrate. However, at higher temperatures, the atoms have kinetic energy and begin to vibrate. This causes the diffraction pattern to be less sharp. It becomes less intense and has added diffuse background scattering.

In order to model these changes, the sample underwent a canonical (NVT) ensemble simulation at the temperature of interest for 110,000 iterations [7]. The NVT is a LAMMPS package that adds a specific temperature and the associated vibrations by time integration on Nose-Hoover style non-Hamiltonian equations of motion which are designed to generate positions and velocities sampled from the canonical ensembles [24]. This updates the position and velocity for atoms in the group each timestep. After 10,000 iterations, we took snapshots every 100 iterations to collect a total of 1000 snapshots. Diffraction patterns were calculated from each of these 1000 diffraction patterns and summed in order to create a more physically realistic data set. This allowed us to see how the atoms in the sample moved.

We then simulated the diffraction based on one of these random images to see if the PRAMMol code could still retrieve the correct average atomic positions in the grain even when the atoms were not perfectly still due to random vibrations. We ran this at every 100 K between 0 K and 1000 K [7].

Chapter 3

Results and Discussion

Using the simulated diffraction patterns, we tested how effective PRAMMol was at recreating the simulated grain structure. These simulations were run using the supercomputers at Brigham Young University [25]. The temperature reconstructions were more accurate than typical phase retrieval methods at similar temperatures. Additionally, they took less time. Further work needs to be done to see if PRAMMol works on real-world data; if so, this code will be able to help with the large amounts of data from updated synchrotrons.

3.1 Temperature Reconstruction

Our PRAMMol algorithm was able to reconstruct the crystals with picometer atomic resolution as shown in Figure 3.1 [7]. Experimentally, this resolution is impossible to achieve for a few reasons, including lattice vibrations due to kinetic energy at higher temperatures. Additionally, we are not really achieving a resolution in a traditional imaging sense, but this is the error in the atomic positions in our model. We tested PRAMMol in more realistic experimental conditions by completing 10 independent reconstruction trials across 10 temperatures for a total of 100 trials.

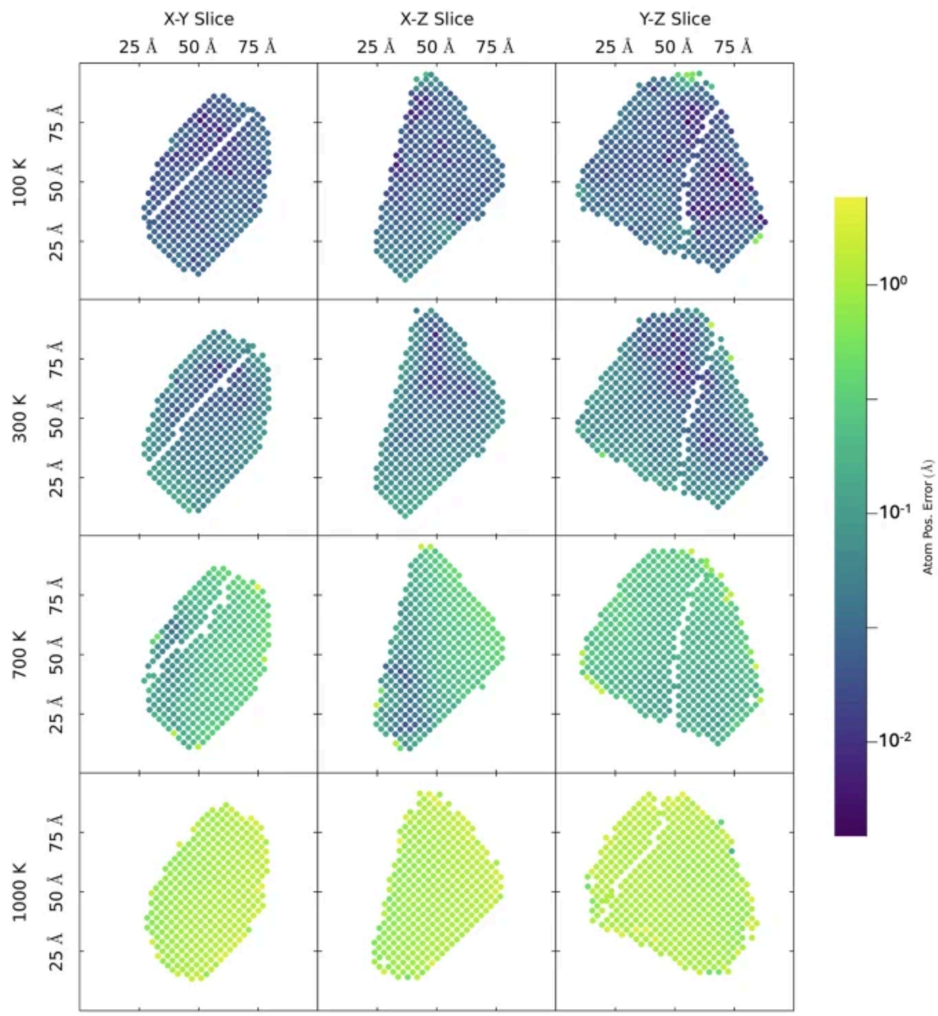

Figure 3.1
Effectiveness of PRAMMol at elevated temperatures. The x-axis shows three different orientations of the same crystal along the x-y, x-z, and y-z planes. The y-axis shows the reconstructions at four different temperatures. The color gradient shows the atomic position error in Angstroms on a logarithmic scale.

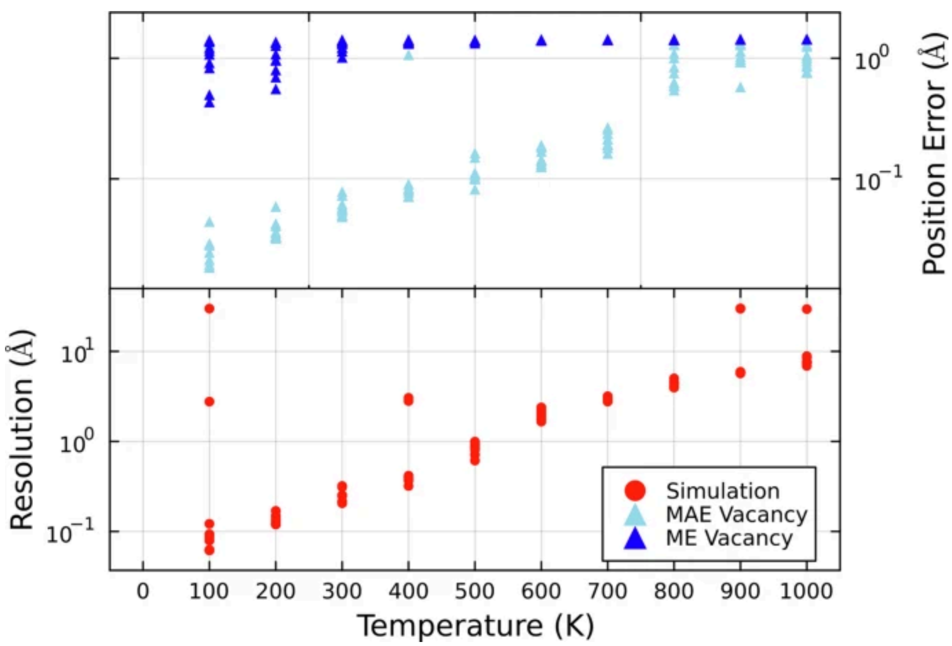

Figure 3.2
Effectiveness of PRAMMol across more temperatures. To assess the PRAMMol in experimental conditions, 10 trials were run across 10 temperatures, for a total of 100 trials. The x-axis shows the 10 different temperatures we ran the trials at in Kelvin. The y-axis on the top panel shows position error — or how far off the atoms are from their correct position — for the mean average error (MAE) and maximum error (ME). The y-axis on the bottom panel shows the resolution of the simulation in Angstroms [7].

As shown in Figure 3.1, PRAMMol was able to reconstruct the interior of the sample. At 100 K and 300 K, PRAMMol effectively reconstructs the entire object at atomic precision except for a few locations on the surface. At 700 K, PRAMMol is still able to reconstruct the original object to high fidelity but occasionally loses atoms. At 1000 K, the object resembles a low-resolution reconstruction that traditional phase retrieval algorithms would output [7]. Overall, PRAMMol began to have errors above 0.5 Angstrom around 700K, and most of the atoms in the 300 K examples had atom errors in the sub 10 pm level (0.1 Angstrom).

To assess the PRAMMol in experimental conditions, 10 trials were run across 10 temperatures, for a total of 100 trials, as shown in Figure 3.2. For temperatures up to 500 K, PRAMMol was able to successfully reconstruct with an error of less than a tenth of an Angstrom below 500 K, and the mean average error of the positions of the atomic reconstruction was beneath a tenth of an Angstrom. Above 700 K, the average atomic position error goes above 1 Angstrom and PRAMMol does not successfully reconstruct the correct number of atoms. Additionally, these trials show that the resolution and mean average error (MAE) are much less than 1 pm and the maximum error is about 1 pm [7]. These results parallel the nanometer resolution of traditional phase-retrieval.

Future work will involve applying this method to real-world data. This will require obtaining three diffraction patterns from a crystal at three different angles. At that point, PRAMMol should be able to reconstruct the original grain if this code is viable for non-simulated data. It will be best to start with a relatively simple grain and then work our way up to more complicated structures, including vacancies and dislocations. This will better allow us to see where system failures initiate on an atomic scale.

Chapter 4

Conclusion

Traditional phase retrieval methods have shown that given enough flux, atomic resolution could be achieved [26]. However, our PRAMMol algorithm has shown that we can retrieve atomic positions to deep sub-Angstrom precision even at room temperature from only three diffraction peaks while bypassing the phase retrieval problem.

This PRAMMol algorithm combines maximum likelihood estimation, atom generation, and cross-validation to successfully recreate grains. In this thesis, we demonstrated PRAMMol efficiency using computer created grains and the associated diffraction patterns. I then modified the grain generation to include vibrations typical at given temperatures. PRAMMol also proved to be successful in simulated grains that included temperature.

The accuracy of the PRAMMol code and its ability to accurately reconstruct simulated data — even as the temperature begins to reach the melting point of gold — demonstrates that this algorithm will be useful on data taken from synchrotrons. This will allow us to take better advantage of the increased photon flux at the upgraded synchrotron facilities. This accuracy is limited by Poisson noise and numerical precision, but we are still achieving near-atomic resolution even with the temperature vibrations included. Specifically, most of the atoms in the 300 K examples had atom errors in the sub 10 pm level and began to have errors above 0.5 Angstrom around 700 K. This is comparable to typical phase retrieval algorithms.

Future work will allow for faster processing and improved temperature modeling and reconstruction. One such demonstration will involve using this code to model data from the upgraded APS synchrotron. This algorithm can also be expanded to include the reconstruction of high-strain data. This will allow for the successful reconstruction of more data and objects [27].

Bibliography

[1] N. Nitta, F. Wu, J. T. Lee, and G. Yushin, "Li-ion battery materials: present and future," Materials Today **18,** 252–264 (2015).

[2] Y. Li, W. Guo, D. I. Stroe, H. Zhao, P. K. Kristensen, L. R. Jensen, K. Pedersen, and L. Gurevich, "Evolution of aging mechanisms and performance degradation of lithium-ion battery from moderate to severe capacity loss scenarios," Chemical Engineering Journal **498,** 155588 (2024).

[3] J. T. Evans, J. P. Evans, R. W. Walker, A. W. Blom, M. R. Whitehouse, and A. Sayers, "How long does a hip replacement last? A systematic review and meta-analysis of case series and national registry reports with more than 15 years of follow-up," Lancet (London, England) **393,** 647 (2019).

[4] A. Khashan, S. Talib, M. Hamouda, J. Kovacs, A. Ibrar, G. Saini, Z. U. Haq, B. Anantharamakrishnan, and M. Alam, "Coronary Artery Stent Dislodgement and Loss in the Bloodstream: A Case Report and Management Options," The American Journal of Case Reports **23,** e937598–1 (2022).

[5] P. Li, M. Allain, T. A. Grünewald, M. Rommel, A. Campos, D. Carbone, and V. Chamard, "4th generation synchrotron source boosts crystalline imaging at the nanoscale," Light: Science Applications 2022 11:1 **11,** 1–12 (2022).

[6] S. Maddali *et al.*, “Concurrent multi-peak Bragg coherent x-ray diffraction imaging of 3D nanocrystal lattice displacement via global optimization,” Npj Comput. Mater. **9,** 1–12 (2023).

[7] J. Meziere, A. H. Carpenter, A. Pateras, R. Harder, and R. L. Sandberg, “Atomic resolution coherent x-ray imaging with physics-based phase retrieval,” npj Computational Materials 2024 10:1 **10,** 1–11 (2024).

[8] W. O. R. Gerchberg Saxton, “A practical algorithm for the determination of phase from image and diffraction plane pictures,” Optik (1972).

[9] J. R. Fienup, “Reconstruction of a complex-valued object from the modulus of its Fourier transform using a support constraint,” J. Opt. Soc. Am. A 4 (1987).

[10] M. Karplus and J. A. McCammon, “Molecular dynamics simulations of biomolecules,” Nature Structural Biology 2002 9:9 **9,** 646–652 (2002).

[11] N. W. Ashcroft and N. D. Mermin, *Solid State Physics* (Holt, Rinehart and Winston, 1976).

[12] P. P. Ewald, “Introduction to the dynamical theory of X-ray diffraction,” Acta Crystallographica Section A **25,** 103–108 (1969).

[13] Y. Gao, X. Huang, H. Yan, and G. J. Williams, “Bragg coherent diffraction imaging by simultaneous reconstruction of multiple diffraction peaks,” Phys. Rev. B **103,** 14102 (2021).

[14] S. O. Hruszkewycz, M. Allain, M. V. Holt, C. E. Murray, J. R. Holt, P. H. Fuoss, and V. Chamard, “High-resolution three-dimensional structural microscopy by single-angle bragg ptychography,” Nat. Mater. **16,** 244–251 (2017).

[15] H. Chang, P. Enfedaque, and S. Marchesini, “Blind ptychographic phase retrieval via convergent alternating direction method of multipliers,” SIAM J. Imaging Sci. **12,** 153–185 (2019).

[16] X. Wei, H. P. Urbach, and W. M. Coene, "Cramér-Rao lower bound and maximum-likelihood estimation in ptychography with Poisson noise," Phys. Rev. A **102,** 043516 (2020).

[17] D. A. Barmherzig and J. Sun, "Towards practical holographic coherent diffraction imaging via maximum likelihood estimation," Opt. Express **30,** 6886–6906 (2022).

[18] M. Grujicic, J. Runt, and J. Tarter, "Molecular Dynamics (MD) and Coarse Grain Simulation of High Strain-Rate Elastomeric Polymers (HSREP): Molecular and Coarse-Grained (CG) Modeling of Shock Wave Mechanics in HSREP," Elastomeric Polymers with High Rate Sensitivity: Applications in Blast, Shockwave, and Penetration Mechanics pp. 187–215 (2015).

[19] S. Arlot and A. Celisse, "A survey of cross-validation procedures for model selection," Stat. Surv. **4,** 40–79 (2010).

[20] P. Hirel, "Atomsk: a tool for manipulating and converting atomic data files," Comput. Phys. Commun. **197,** 212–219 (2015).

[21] A. P. Thompson *et al.*, "LAMMPS - a flexible simulation tool for particle-based materials modeling at the atomic, meso, and continuum scales," Comput. Phys. Commun. **271,** 108171 (2022).

[22] S. J. Plimpton and A. P. Thompson, "Computational aspects of many-body potentials," MRS Bull. **37,** 513–521 (2012).

[23] Y. Mishin, D. Farkas, M. J. Mehl, and D. A. Papaconstantopoulos, "Interatomic potentials for monoatomic metals from experimental data and ab initio calculations," Phys. Rev. B **59,** 3393–3407 (1999).

[24] S. Corporation, "fix nvt command — LAMMPS documentation,", 2003.

[25] BYU, “Office of Research Computing - BYU,”.

[26] S. H. Dietze and O. G. Shpyrko, “Coherent diffractive imaging: towards achieving atomic resolution,” J. Synchrotron Radiat. **22,** 1498–1508 (2015).

[27] J. Meziere, S. Mohan, B. Bekker, H. Oliver, L. Cvetko, A. P. Stebner, and G. L. Hart, “Structural determination of a cubic Ni-rich phase in Hf-Ni-Ti,” Acta Materialia **287,** 120748 (2025).

Index